Voronoi D2RP and AI D2RO System Potential

Aashna Singh - Anaelle Mathieu - Ilai Debazi - Luca Marchetti - Niels Koenraad - Sohyun Park

[1] The Faculty of Architecture and the Built Environment, Delft University of Technology
[2, 3] Henriette Bier, Arwin Hidding

Table of Contents

1. Abstract

This paper investigates how Design-to-Robotic-Production (D2RP) and Design-to-Robotic-Operation (D2RO) can be combined to improve inhabitation conditions within the constrained interior of the Troll Research Station in Antarctica. On the production side, the project develops a parametric spatial system based on Voronoi geometry, chosen for its scalability, editability, and compatibility with robotic 3D printing with recycled plastic. Rather than treating Voronoi as a purely expressive formal language, the research controls it through seed-point organization, combining irregular and orthogonal logics within one continuous field. Orthogonality is introduced where usable surfaces are required, while buffer zones enable smooth transitions between ordered and non-ordered regions in both 2D and 3D. Openings, furniture objects, and circulation vectors act as inputs that inform the final container layout, producing a generative design tool capable of diverse and personalized spatial outcomes. On the operational side, the project develops an AI-supported lighting system in Python with three objectives: circadian rhythm preservation, personalized physiological response, and environmental energy optimization. The model is trained on two data groups—weather data from De Bilt and a synthetic physiological dataset—and predicts lighting intensity and correlated colour temperature to simulate Delft daylight cycles inside the container while adapting to biometric markers. To reduce overfitting, correlation analysis was used to remove redundant features before training an MLP regressor, whose performance was evaluated through R-squared, MAE, and RMSE. The system was further visualized through a Streamlit interface integrating both numerical outputs and the Voronoi-based spatial model. Together, the research proposes a responsive architectural framework in which spatial reconfiguration and adaptive lighting operate as one coherent system for extreme environments.

Keywords: Voronoi, Artificial Intelligence, Lighting, Extreme environments

2. Introduction

Extreme environments often present significant challenges for human inhabitation. Whether in the deep ocean, outer space, or polar regions, a primary concern remains preserving human's physical and mental health over extended periods of isolation. In these contexts, architecture is fundamentally limited by logistical and environmental constraints resulting in small, dense, and confined spaces which do not respond to the physiological and psychological requirements of the inhabitants living in these extreme environments.

The Troll Station in Antarctica is one such case where prolonged confinement within a small, static container intersects with extreme polar weather and abnormal light cycles producing significant challenges to the health of the researchers that inhabit it year round. The narrow interiors of the station force researchers to conduct all activities from work to rest to socialising within an extremely limited footprint. Additionally, months of continuous darkness during polar winter followed by continuous daylight during the summers severely disrupt circadian rhythms, sleep patterns, hormone regulation and mental health.

To address the challenges of confinement and static lighting, this paper explores two complementary design strategies through a Voronoi-based D2RP, Design to Robotic Production, and AI supported D2RO, Design to Robotic Operation. The first design strategy employs a Voronoi based computational approach to generate reconfigurable furniture designed for the changing user needs to accommodate various activities. The Voronoi based system enables each user to customize their own space by adjusting the size, location, and density of furniture elements according to personal needs, resulting in a dynamic container which gives more agency to the researchers. The second design strategy applies Artificial Intelligence to dynamically adjust the lighting in the interior through the simulation of a 24 hour light cycle during long winters and a personalized physiological response that uses biometric markers, such as heart rate, to tailor lighting conditions to each researcher.

This research paper utilizes the case study of one container, 6/2.5/2.5m, housing two researchers at the Troll Station and providing spaces for sleeping, resting, working, and socialising. The strategies are developed within the framework of additive 3D printing using recycled plastic ensuring that material waste is minimised. Together, the two design strategies, Voronoi furniture and AI Lighting, demonstrate the potential of transforming confined polar and extreme habitats into responsive and healthy environments for users that inhabit them for extended periods of time.

3. Methodology Part 1: Voronoi-based D2RP

3.1 Voronoi diagrams

Voronoi is a way of organising space through proximity. Starting from a set of points, it divides a field into cells, each defined by the area closest to one generating point. The resulting pattern is not arbitrary: its boundaries emerge from the relation between points and shifts as those points are moved, added, aligned, or spaced differently. Voronoi is therefore useful not simply as a visual motif, but as a rule-based system in which form can be steered through the placement of points. [1]

This makes it especially valuable in design processes that require both variation and control. Rather than drawing every edge directly, the designer works indirectly by adjusting the underlying point structure, allowing differentiated spatial conditions to emerge from one coherent logic. [2]

3.2 Why Voronoi?

The choice of Voronoi as the primary spatial system for this project responds to three interconnected concerns: materialization, production, and form.

In terms of materialization, the project works with recycled plastic at Troll Station as its primary material, addressing circular design at both a conceptual and practical level. Voronoi geometry is structurally well-suited to this choice: the cellular network distributes loads efficiently across a continuous lattice, reducing material waste while maintaining structural integrity. This makes it compatible with a circularity-driven approach, where the amount of material used and its potential for recovery after use are both considered from the outset.

In terms of production, the Voronoi system is particularly well-adapted to robotic 3D printing workflows. The continuous and mathematically describable nature of the tessellation means that toolpaths can be generated directly from the geometry without manual intervention. Crucially, the faceted character of Voronoi cells also provides a logical basis for integrating wiring and LEDs during the printing process: the planar faces of each cell become sites for embedding light-emitting elements, so that the lighting system is not added as a separate layer but is structurally woven into the printed material itself.

In terms of form, the use of Voronoi responds to a fundamental spatial problem posed by the container context at Troll Station. A standard shipping container is a rigid, rectilinear volume with little inherent spatial differentiation. Voronoi offers a way to articulate that interior into zones of varying density, scale, and character without introducing conventional walls or partitions. The resulting spatial system is differentiated, it can accommodate distinct programs such as sleeping, working and lounging, while remaining formally continuous and reconfigurable. Rather than subdividing space through fixed elements, Voronoi inflects it.

Finally, the complexity and interdependency of these three concerns made a scripted approach necessary. The project required a single tool capable of holding multiple variables in relation simultaneously: the dimensions and placement of furniture elements such as beds, desks, and

shared spaces; the size and position of openings; the density and character of the Voronoi field; and, crucially, the integration of lighting directly into the printed cells. None of these parameters can be treated in isolation; a change in furniture layout affects the void structure, which affects the tessellation, which affects the surfaces available for LED integration. A manual process could not manage this interdependency across the full range of configurations the design needed to support. The Grasshopper script was therefore developed not to produce one fixed outcome, but as a reconfigurable design tool: one coherent system that adapts to different users, programs, and spatial conditions while maintaining the geometric and fabrication logic throughout.

3.3 Controlling the Voronoi through seed-point organization

The geometry of a Voronoi diagram is not defined by drawing cells directly, but by placing points. In a standard Euclidean Voronoi diagram, each cell contains all locations closer to one seed point than to any other. The boundaries between cells are therefore defined by the relations between neighbouring seeds, meaning that the spatial outcome of the tessellation is determined primarily by how the seed points are arranged before tessellation begins. The Voronoi operation does not invent form independently; it makes an underlying point distribution spatially legible.

In this project, that dependency on point distribution became the main design lever. Rather than developing two separate Voronoi systems, the script operates through a single field controlled by different logics of seed placement in different regions of the space. One is an orthogonal point logic, in which seed points are arranged on a regular grid of 25 × 25 cm. This module was selected because it divides evenly into the container dimensions of 6.00 m in length and 2.50 m in width and height, allowing the grid to organise the interior without remainder. This ordered distribution produces a more controlled and legible tessellation, with more even cells, more predictable boundaries, and clearer responses to architectural constraints such as wall edges, openings, and furniture alignments.
Its importance became clear once the project moved from geometric exploration to the spatial needs identified through the 24/7 mapping of the overwintering crew at Troll Station. That mapping revealed five key programs to be accommodated: shared space, sleeping, lounging, individual work, and storage. Most of these depend on flat, stable, and usable surfaces, such as beds, tables, and shelves, which do not emerge reliably from an irregular Voronoi field alone. Orthogonality therefore became a functional requirement rather than a formal preference. By aligning seed points on a regular grid, straighter boundaries and more usable surfaces could be produced where the design required spatial clarity and practical occupation.

The second is a non-orthogonal point logic, in which seed points are distributed through stochastic or semi-random population methods. These irregular distributions introduce local variation, asymmetry, and a less mechanical character into the field. Where the design benefits from spatial complexity, visual differentiation, or a more organic appearance, such as in the structural shell or transition zones between programs, this looser seeding logic allows the tessellation to diversify without breaking from the same underlying system.
The key point is that these are not two separate Voronoi diagrams, but two ways of seeding one continuous field. By shifting between ordered and stochastic point placement, the spatial character

of the interior can be modulated gradually, allowing the design to move between regularity and variation within one coherent geometric logic.

3.4 From 2D principles to 3D implementation

Having established the need for usable surfaces, the next challenge was to generate them within the Voronoi logic itself. Rather than abandoning the system, its control points were manipulated to produce straighter and more regular boundaries. In the 2D studies, this resulted in diagrams with horizontal edges, showing that flat surfaces could emerge through controlled point placement. These experiments established the geometric principle later transferred into the 3D script, where the control points were arranged accordingly to generate a spatial configuration with integrated flat surfaces. Figure xy illustrates this behaviour by comparing irregularly placed control points with points arranged on a raster, showing how the latter produces straighter and more usable boundaries.

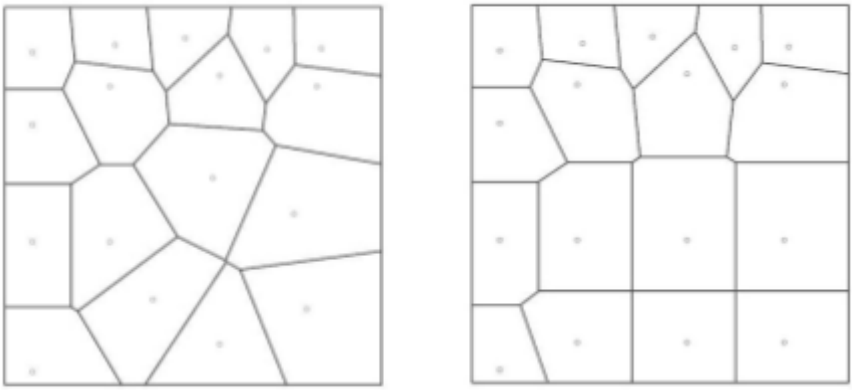

Fig. 1: Comparison between voronoi diagram created by irregularly placed control points and points arranged on a raster

3.5.1 Buffer zones as a control mechanism

To understand how an orthogonal grid and a Voronoi grid can be merged, a clear strategy must first be defined. This strategy is guided by three primary objectives. First, it must preserve the orthogonal grid so that its inherent qualities and underlying logic remain intact. Second, it should establish a transition between the orthogonal grid and the Voronoi structure. Third, it must stabilise and maintain the geometry around specific predefined constraints.

To address these requirements, a buffer zone is introduced. This buffer zone is essential for enabling a controlled transition between the two systems. It operates between a predefined constraint, represented as a rectangle populated with an orthogonal grid, and the surrounding of the non grid structured voronoi.

The buffer zone functions by increasing the density of points in the area surrounding the constrained region. This higher point density creates a protective layer around the orthogonal grid. As a result,

the orthogonal grid does not directly connect to the Voronoi structure, allowing the system to meet all three of the predefined objectives.

3.5.2 2D Buffer zone around windows

To understand how this system operates, it is useful to first consider a two-dimensional simplification. The initial step is to define the location of the window. This location remains constant, regardless of variations in furniture distribution or sizing. This is because the windows are not secondary additions to the container, but integral elements of its physical walls. Consequently, a buffer zone is introduced to ensure that the window position and approximate size remain consistent across different configurations.

Fig. 2: Defining Boundary conditions


Fig. 3: Population of grid points

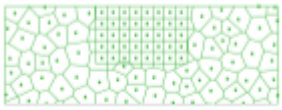
Fig. 4: Surrounding voronoi

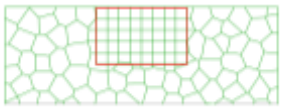
Fig. 5: exceedance of boundary

The process begins by defining the window location and its maximum dimensions (see Figure 2). A two-dimensional rectangle representing this maximum window size is then populated with an orthogonal grid with a spacing of 0.25 m (see Figure 3). If this orthogonal grid were directly connected to a Voronoi point cloud, the transitional cells between the orthogonal and Voronoi structures would extend beyond the boundary of the maximum window size (see Figures 4 & 5).

To prevent this, a buffer zone of points is introduced. This buffer zone is generated by creating a gradient in point density, allowing the dense orthogonal grid to transition smoothly into the less dense Voronoi structure. Specifically, four concentric layers are constructed around the maximum window boundary (see Figure 6), with each successive layer decreasing in point density as the distance from the window increases (see Figure 7).

Fig. 6: Creating offsets


Fig. 7: Populating with density gradient


Fig. 8: Culling inside points

Following this, all points within an inward offset of 0.125 m are removed. This value corresponds to half the dimension of the orthogonal grid cell, ensuring that the orthogonal grid remains minimally distorted. The resulting point cloud (Figure 8) forms the buffer zone between the two systems.

Finally, the three distinct point clouds are merged: (1) the orthogonal grid, (2) the buffer zone, and (3) the Voronoi structure (Figure 9). The end result is illustrated in Figure 10. This approach produces a system that enables a smooth transition between the Voronoi and orthogonal grids, while preserving both the integrity of the orthogonal grid and the maximum window dimensions. This is particularly important, as the transitional cells along the boundary of the window allow it to be consistently integrated across a wide range of Voronoi configurations,

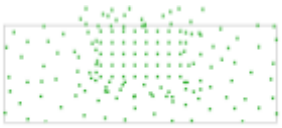
Fig. 9: Combining point clouds


Fig. 10: End result

which may vary significantly depending on individual furniture arrangements.

3.5.3 Buffer zones around furniture

A similar strategy is applied to the furniture elements within the system. To ensure that furniture boxes retain their intended dimensions, buffer zones are introduced around each predefined furniture boundary. Without such a buffer, directly connecting the orthogonal grid associated with the furniture to the surrounding Voronoi structure would result in oversized transitional cells. These irregular in-between cells can significantly distort the geometry, causing the resulting furniture dimensions to deviate from their original specifications.

To prevent this, each furniture box is treated as a constrained region, comparable to the window condition. An orthogonal grid is defined within the bounds of the furniture geometry, after which a surrounding buffer zone is generated.

By introducing this buffer, the system preserves the intended size and proportion of the furniture elements while still allowing them to integrate into the larger Voronoi-based structure. This ensures that, regardless of variations in the overall configuration, the furniture remains consistent and functionally reliable within the spatial system.

3.6 Defining the void

As introduced in the previous section, orthogonally configured furniture and openings collectively react to surrounding space, expressed through 3D ordered and irregular Voronoi cells. However, securing sufficient voids is indispensable to ensure these space's function.

In this context, the void space can be classified into two categories:

1) Void for ensuring the functional usability of furniture such as lounges, chairs, and beds.
2) Void for circulation which connects furniture elements with openings such as doors and windows.

Distinct systematic approaches are necessary because of the differing functional requirements. The section will explain the methodologies for generating these voids and the process of removing corresponding cells from the 3d Voronoi cells.

3.6.1. Void for Furniture Usage

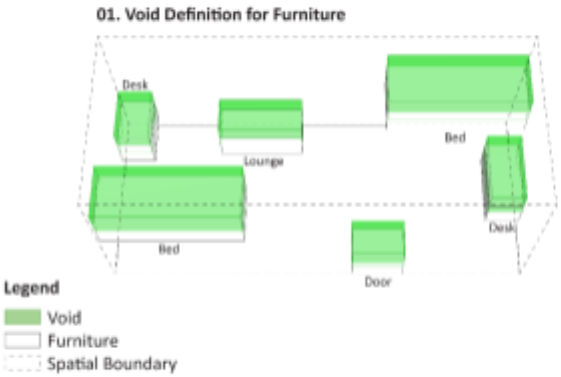


Process of Defining Voids for Furniture

Fig. 11: Process of defining Furniture-based void

Furniture elements are constructed using an orthogonal system based on a 0.25m modular unit, and are categorized into beds, lounge, and chairs. These furniture elements require sufficient overhead clearance for proper usability.

The project defines sufficient overhead volumes for the furniture elements by extracting the upper surface and subsequently extruding into the Z-axis.

In the Grasshopper, the process is implemented as follows.

Firstly, the furniture geometries are deconstructed using the Deconstruct Brep function to extract individual surfaces. Secondly, use the Area function to determine the centroid of each surface. Thirdly, find the uppermost surfaces by decomposing these centroid points and sorting them based on their Z-coordinates. Lastly, extrude the selected surfaces vertically to a predefined height, and generate the void having sufficient overhead height for furniture usages.

3.6.2. Void for Circulation, between furniture and openings

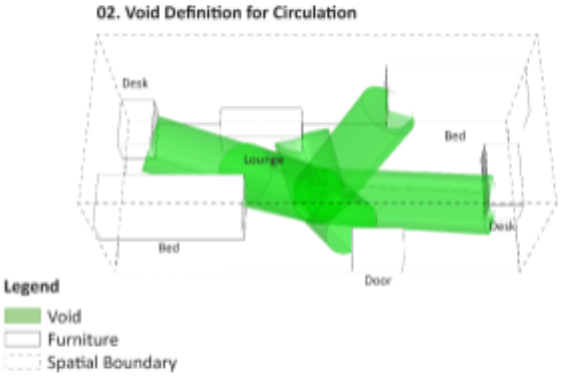

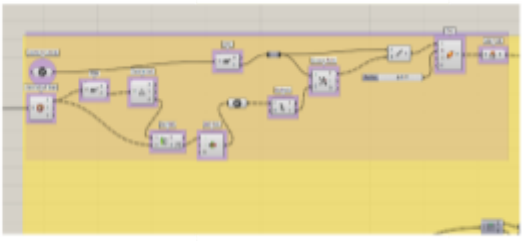
Process of Defining Voids for Circulation

Fig. 12: Process of defining Circulation-based void

In addition to furniture usability, allocating void spaces is also required to support user movement between furniture and openings. To achieve this, circulation paths are defined based on the shortest connections between elements.

A reference point located at the center of the container floor surface is selected as the main connection, as the project designates the central area as an open space. Then, shortest paths are generated using the Closest Point function to establish a linear connection.
Subsequently, these lines are transformed into volumetric geometries through the Pipe function with a sufficient radius to accommodate human movement. This generates voids for circulation that represent accessible pathways within the spatial system.

3.6.3. Collision Detection and Cell Culling

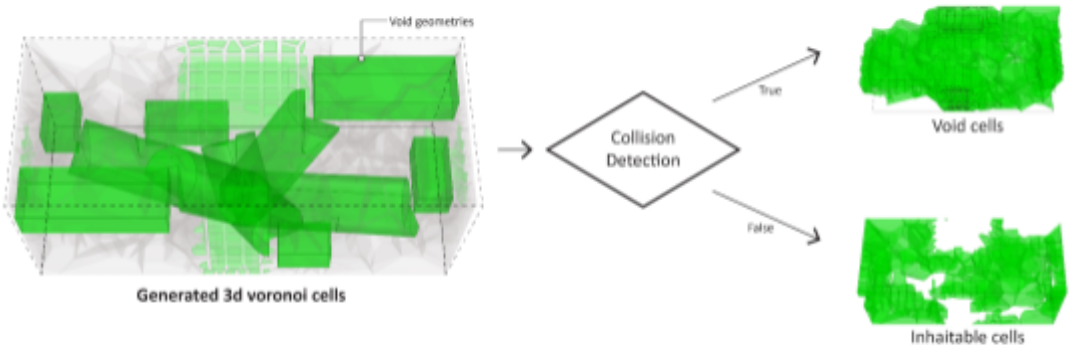

Fig. 13: Void cell selection through collision detection function

The void geometries for furniture usage and circulation are aggregated into a single list to detect their spatial collision with the 3d Voronoi cells.
Intersections between each Voronoi cell and the void geometries are detected by using the Collision One/Many function in the grasshopper. The output is exported in a Boolean list such as [1,0,0,1,1,...], where intersecting cells are printed as True [1] and non-intersecting cells as False [0]. This list corresponds directly to the indexed set of generated 3d Voronoi cells.
By inputting this boolean pattern into the Cull index function, the intersecting cells can be selectively removed resulting in a refined set that will define the void region. Conversely, the inhabitable region can also be selected by inverting the boolean pattern.
Through this process of void definition and selective cell removal, the 3D Voronoi system is adapted to accommodate both furniture usability and human circulation.

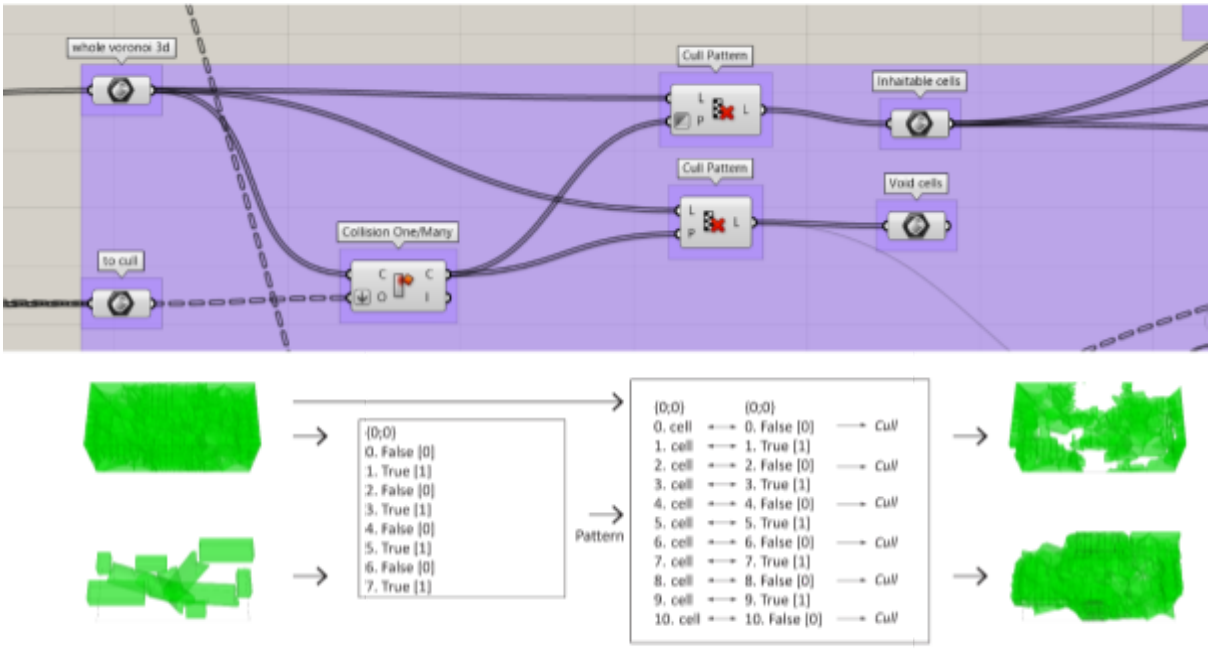

Fig. 14: Process of collision detection and cell culling

3.7. Output of the script: a reconfigurable design tool

Following the previous processes, the script produces an optimized configuration of private space. Rather than functioning as a tool for generating a single monolithic form, it operates as a generative design system capable of producing diverse spatial outcomes.

By adjusting the size and location of opening, composition of furniture elements, and density of the Voronoi cells, users enable to generate the optimized space having a different spatial system and density.

Such variability enables a flexible spatial configuration independent of specific users or programs, while allowing for reconfiguration in response to diverse usage scenarios.

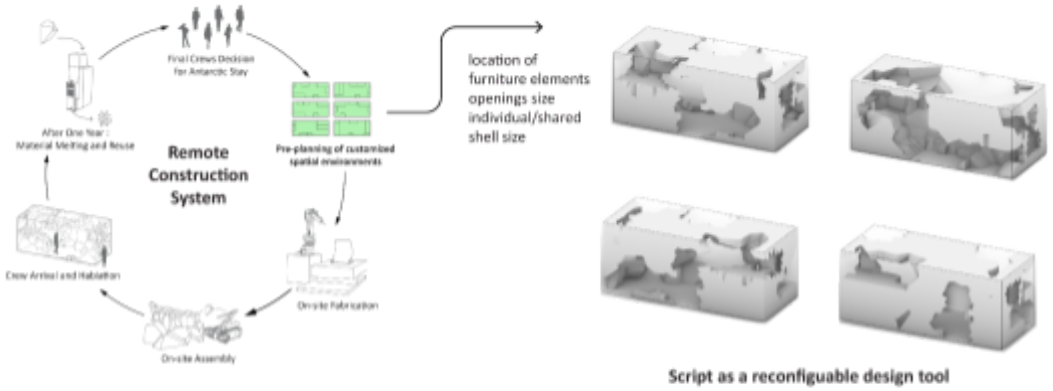

Fig. 15: Remote Construction Workflow and Parametric Spatial Configuration Tool

4 AI Supported D2RO (Digital Intervention)

The Antarctic lighting cycle presents significant challenges to the human body. At the Troll Station, the overwintering staff endure polar nights with months of complete darkness followed by summers of continuous daylight. This extreme oscillation disrupts circadian rhythms, impairs sleep, and negatively affects psychological health. To address this challenge, the static and tunable lighting commonly used in remote stations cannot adequately respond to the body's changing needs or the extreme external conditions. With the introduction of artificial intelligence in lighting, the container lighting can dynamically adjust color temperatures, intensity, and timing based on real time environmental and biometric feedback. This thereby creates a significantly healthier physiological and psychological environment for the research staff at the Troll Station.

4.1 Performance goals

There were three primary objectives with the AI integration: Circadian rhythm preservation, personalised physiological response, and environmental energy optimisation. The goal of all three objectives was to create a more personalized system that regulates the human body physiologically and psychologically while optimising energy efficiency.

The human body's circadian rhythm is controlled by a biological clock, composed of a group of nerve cells that form a structure called suprachiasmatic neurons (SCN) which controls the production of hormone melatonin based on the amount of light the eyes receive. [3] Disruption to the circadian rhythm can lead to lower hormone secretion which affects sleep cycles, the immune system, and mental health. [3] Due to long periods of darkness in the Antarctic region along with polar nights, the human body's natural circadian rhythm is disturbed which can cause long term physiological damage to the over-wintering staff at the Troll Station. [4] Numerous studies suggest that artificial lighting, a blue light with a high lux, during winter in the polar regions can reduce some of the damage caused by the dysregulated circadian rhythm and can help improve sleep and performance throughout the day. [4] Although colder light temperatures and higher lux levels can be easily implemented at the Troll station, the research aimed to automatically simulate a 24-hour cycle based on a typical city like Delft through artificial lighting. With the use of artificial intelligence, this process is highly optimized and allows for the simulation of natural daylight variations throughout the year.

To further support human physiological regulation, biometric markers such as heart rate, blink rate, and respiratory rate could be used to dynamically adjust artificial lighting creating a more responsive system for each individual. Various studies have indicated that exposure to different color temperatures or lux can have a significant effect on some of the biometric markers and can simulate a specific physiological state or mood such as calm or alert. One such study signifies that warmer LED lighting can lower the LF/HF ratio of the heart rate variability and simulate a more relaxed state in the nervous system while colder LED lighting led to the opposite by increasing the higher sympathetic activation creating a more alert and stressed state. [5] The aim of integrating these biological markers to control the artificial lighting inside the container was to respond to the occupant's physiological cues enhancing their well-being and mental state. Artificial intelligence is then used to continuously interpret these markers and adjust lighting in real time. In the case of the Antarctic region, it is particularly useful as the occupants of the Troll Station are regularly exposed to extreme temperatures which cause significant spikes in their biological markers. This dynamic lighting system

aids faster recovery from those conditions and helps regulate the human body back to the interior environment with reduced stress levels.

Beyond the two physiological controlled lighting objectives, the aim was also to introduce energy efficiency within those systems. Due to limited resources in Antarctica, it was important to ensure the system operated efficiently while maintaining the personalized needs of the occupants. The intention was for the system to use the weather data, such as total cloud cover or global illumination levels, to automatically modulate light levels according to the changing conditions. For example, if total cloud cover is low, the interior lighting will automatically dim in response to the brighter environment. Through the use of Artificial Intelligence, this system is dynamically responsive to the exterior conditions and changes in real time.

4.2 Computational Framework: Supervised Learning & Data Synthesis

To achieve the three objectives, a supervised learning workflow was developed in Python. Supervised learning refers to a type of artificial intelligence where a model is trained on input data that has been labelled for a certain output. The model then identifies patterns between the input and output labels allowing for it to accurately generate results when confronted with unexplored or new data. [6] The aim was to train the machine learning model with the weather and physiological data and output lighting temperature and levels predicted through that data. For this study, two different data sets, weather and physiological, were used to train the model.

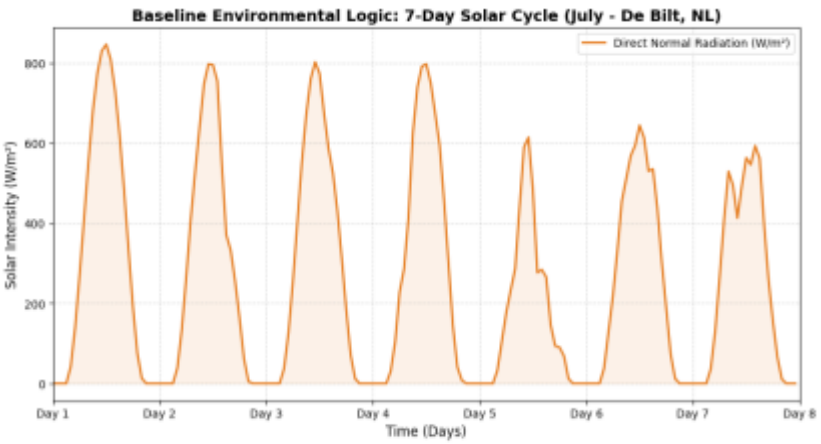

Fig. 16: De Bilt, Netherlands 7 day solar cycle

The longitudinal weather data was derived from KNMI (Royal Netherlands Meteorological Institute) in De Bilt, Netherlands [7] providing a highly accurate dataset for the model to be trained on. The main features, inputs, assumed to influence the light levels were direct normal radiation, diffuse normal radiation, global horizontal radiation, direct normal illumination, diffuse horizontal illumination, global horizontal illumination, outdoor temperature, relative humidity, infrared radiation and total sky cover. Figure 16 shows the seven day solar cycle in the month of July reflecting the total maximum and minimum solar intensity on each day in De Bilt. This graph represents what light levels might look like inside the Troll station container if a July day was simulated.

For the physiological data, a synthetic data set was used to train the model including the features, inputs, as HRV rmssd ms, heart rate, skin conductance, respiratory rate, pupil diameter, and blink rate. Although a synthetic data set was used to train the model initially, it provided a baseline, with the goal of later integrating smart watch data from the occupants of the Troll Station for more precise learning. Table 1 shows the synthetic data set used to train the machine learning model on the physiological features.

timestamp	hour	illuminance_lux	sol_beta	sol_label	hrv_rmssd_ms	heart_rate_bpm	pupil_mm	blink_rate_per_min	skin_conductance_uS	respiratory_rate_bpm
9-12-2025 00:00	0	993.8	3843	neutral	55.8	64.3	6.17	15.6	0.31	13.1
9-12-2025 00:05	0	917	3787	neutral	56.3	61.2	6.65	14.8	0.33	15.2
9-12-2025 00:10	0	812.4	3804	cool	52.2	64.2	5.84	16.2	0.38	14.7
9-12-2025 00:15	0	1205	3893	cool	52.8	66.4	4.46	12	0.82	17
9-12-2025 00:20	0	537.2	3822	soft warm	58.8	60.7	6.46	16.4	0.25	15.1
9-12-2025 00:25	0	505.9	3816	soft warm	60.9	61.7	6.79	15.7	0.31	14.8
9-12-2025 00:30	0	979.9	4079	cool	48.1	66.4	5.83	13	0.83	15
9-12-2025 00:35	0	653.9	3952	neutral	56.4	63.8	6.62	16.3	0.33	15.1
9-12-2025 00:40	0	806.7	3858	cool	44.1	62.4	5.39	11.9	0.71	14.7
9-12-2025 00:45	0	1214.1	4811	daylight	40.3	67.3	5.29	10	0.87	16.7
9-12-2025 00:50	0	979.1	3873	cool	52	63.8	6.85	16.5	0.32	14.3
9-12-2025 00:55	0	1467.9	5868	daylight	34.2	66.8	4.89	12.1	0.88	16.2
9-12-2025 01:00	1	1281	4957	daylight	39.4	67.4	4.53	11.9	0.87	15.3
9-12-2025 01:05	1	934.9	3758	cool	50.9	64.5	6.84	19	0.33	13.4
9-12-2025 01:10	1	909.5	3443	neutral	52.8	61.9	6.37	16	0.26	13.7
9-12-2025 01:15	1	802.3	4074	cool	46.2	65.9	5.33	16.2	0.55	14.5
9-12-2025 01:20	1	1045.5	4058	daylight	43.8	65.6	5.2	14.5	0.5	14.7
9-12-2025 01:25	1	896.7	3768	neutral	50.7	63.1	6.61	15.8	0.35	13.1
9-12-2025 01:30	1	1307.7	4898	cool	52.1	66.1	5.87	11.7	0.88	15
9-12-2025 01:35	1	973.6	3461	neutral	61.8	66.4	6.67	17.4	0.27	14.8
9-12-2025 01:40	1	949.6	3811	neutral	61.8	64	6.66	17	0.17	15.4

Table 1: Synthetic dataset for physiological markers

Following the selection of the datasets, a correlation analysis was conducted through the creation of scatter maps to prevent overfitting in the machine learning model. Overfitting occurs when the model cannot generalize well from the observed data due to the presence of noise, limited size of training set, and complexity of classifiers. [8] To prevent overfitting, a series of scatter maps are created from the datasets to show correlations and eliminate redundant data/features while training the model for accuracy. In preparation for the scatter maps, the data was grouped based on the hypothesis that similar features would exhibit similar patterns. Figure 17 shows the groups divided based on their similarities: Solar radiation features, visible light features, atmospheric conditions, physiological stress indicators, and eye response metrics.

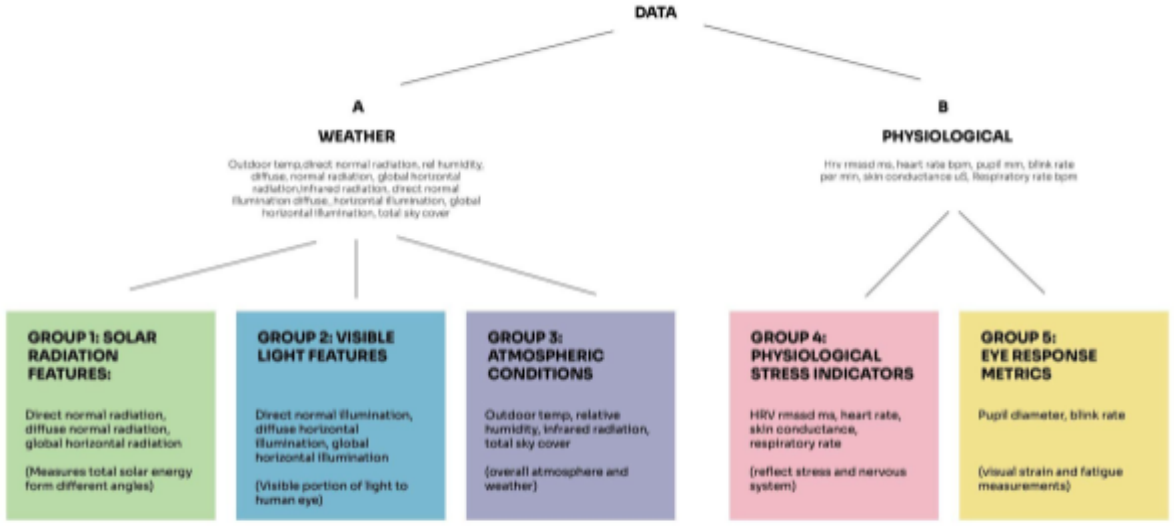

Fig. 17: Data grouping according to similar features

Each feature from these groups were then plotted against each other in the scatter map to explore potential correlations. Figure 18 shows two of those scatter plots: the left plot between heart rate and respiratory rate as a positive correlation and the right plot between hrv rmssd ms and respiratory rate as a negative correlation. The positive correlation indicates that the features are closely related, suggesting that one could be omitted during the training of the model, whereas the negative correlation implies the opposite. Figure 19 illustrates all the scatter maps plotted against each other to show the patterns between the data. The hypothesis was confirmed for most groups, which exhibited similar patterns, however in some groups, multiple features were retained. The final features (input) chosen to train the model were: Direct normal radiation, direct normal illumination, outdoor temperature, total sky cover, hrv rmssd ms, heart rate, skin conductance, and pupil size.

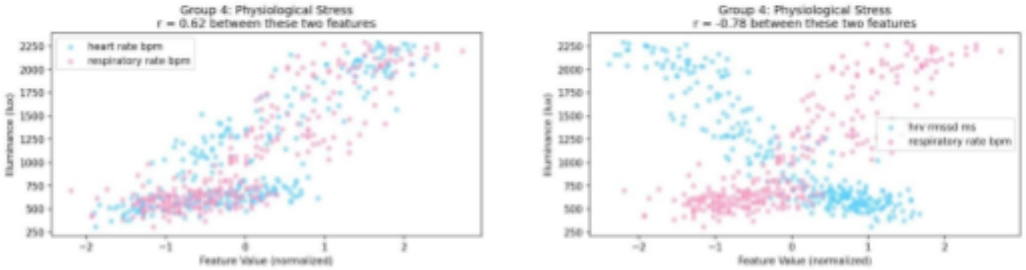

Fig. 18: Scatter diagrams showing the correlation between heart rate bpm, respiratory rate, and hrv rmssd ms

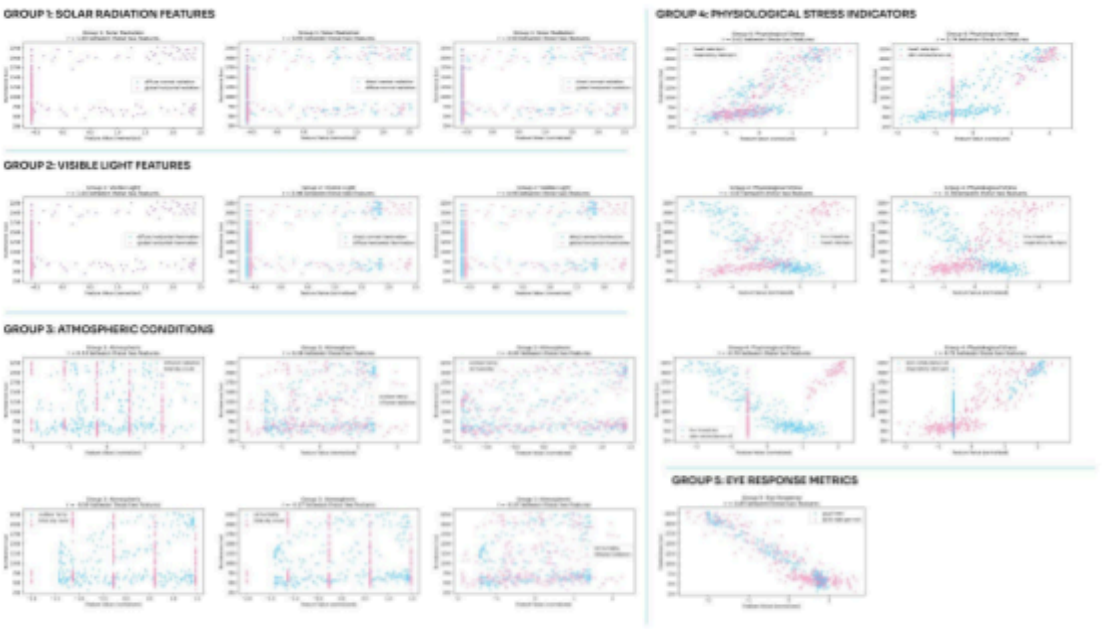

Fig. 19: Scatter plots highlighting correlations and variations among all groups.

After final feature selection, the model is then trained through the MLP (Mulit-layer Perceptron) Regressor function from Sci-Kit Learn library. MLP Regressor is a machine learning model based on a non-linear function and maps inputs to outputs by training on a dataset. [9] The dataset was partitioned into a 70/30 split allowing for the training to utilize 70% of the given data while the remaining 30% utilized unseen data to test predictions. This step trains the model for inference,

which is the stage where the model applies the learnt patterns to new, unseen data. [10] The model is then trained utilizing these parameters.

4.3 Model Evaluation and Accuracy

The accuracy of the model was evaluated through three different parameters: R-squared, the co-efficient of determination, mean absolute error (MAE), and the root mean squared error (RMSE). R-squared is a metric gauging the accuracy of the model through capturing the variance in the data, ranging from 0 to 1, where values closer to 1 indicate a better fit. [11] Values above 0.80 often indicate that the model is quite precise and has good predictive performance. The model that was trained for this study was shown to have an R-squared value for illuminance of 0.9636, which indicates that the model explains 96% of the variance in the data, suggesting a strong fit. Meanwhile, the R-squared value for CCT was 0.8595 suggesting that the model was a strong fit, however, it could still be improved.

The mean absolute error (MAE) is a measure of the average difference between the predicted values and actual values in regression, in units such as lux or kelvin. While, the root mean squared error (RMSE) is more sensitive to outliers and often detects spikes in the system more than MAE. [12] While a model is considered to be high performing when the R-squared reaches closer to the value of 1, with MAE and RMSE, as the value reaches closer to the 0, it indicates there are lower errors in the prediction. For the model in this study, the MAE for illuminance was 86.36 and CCT 242.08, which suggests that the model's prediction deviate by 86 lux and 242 kelvin from the target values. These deviations are relatively low and not entirely perceptible to the human eye. Additionally, the RMSE for illuminance was 112.48 and CCT 335.23, reflecting a deviation of 112 lux and 335 kelvin.

While these values indicate that the model is highly accurate, there are limitations to this as a synthetic data set was used to train the model for physiological data. For a limited study such as this, the model performs well, however, to implement this model into the Troll Station, the model will need to be trained on real-time data from the occupants to be able to simulate desired lighting conditions.

4.4.1 Visualisation of ML model

The final stage of the computational framework was to visualize and create a responsive control interface to be able to test the trained model. This study utilized Streamlit, an open source framework that allows for creation of web applications through Python. The development of this web app was supported by AI-assisted coding, Anthropic's Claude Code, which facilitated the integration of the machine learning model into the responsive control interface.

The web app contains three different tabs: Daylight simulation, energy saving, and physiological control. The daylight simulation tab allows for the occupants to pick any day and hour from the data, and simulates what the lux and kelvin would be. In Figure 20, a simulation of June 4, 2025 at 7:00 am can be shown to have 3471 kelvin and 626 lux. The model also recognizes what the mental state of the occupant will be according to the lighting, with the prediction being 'relaxed focus' in this specific case.

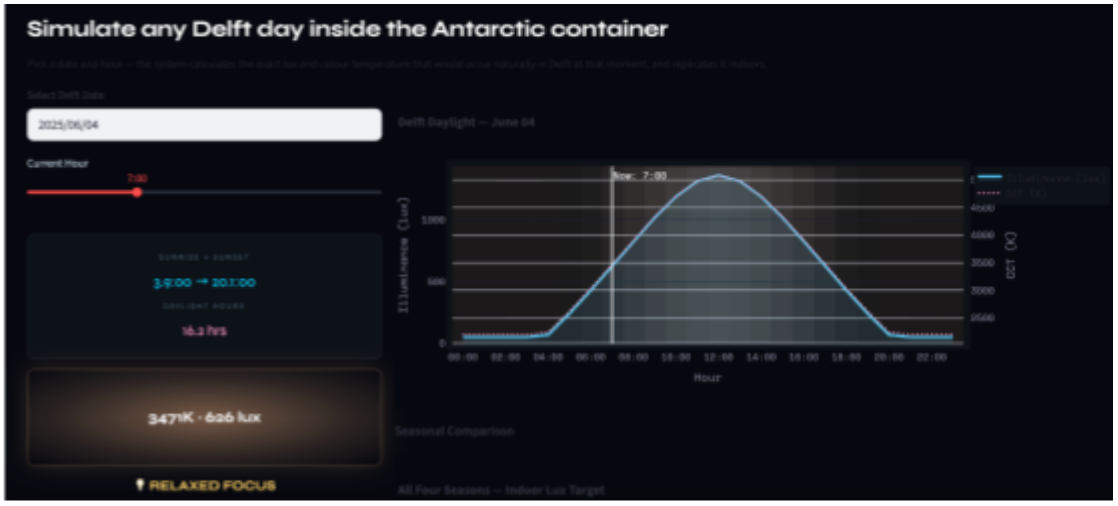

Fig. 20: Website showing weather data simulation tab

The energy saving tab controls the illumination and simulates through sliders the different outputs the model would predict according to the outdoor conditions. Figure 21 illustrates that when the direct solar radiation is 610 W/m^2 , the cloud cover is 3.50 oktas, outdoor temperature is -26C, and relative humidity is 60%, the model predicts that the indoor lux should be 763 lux, which saves about 67% of energy based on the simulated June day used in Figure 20.

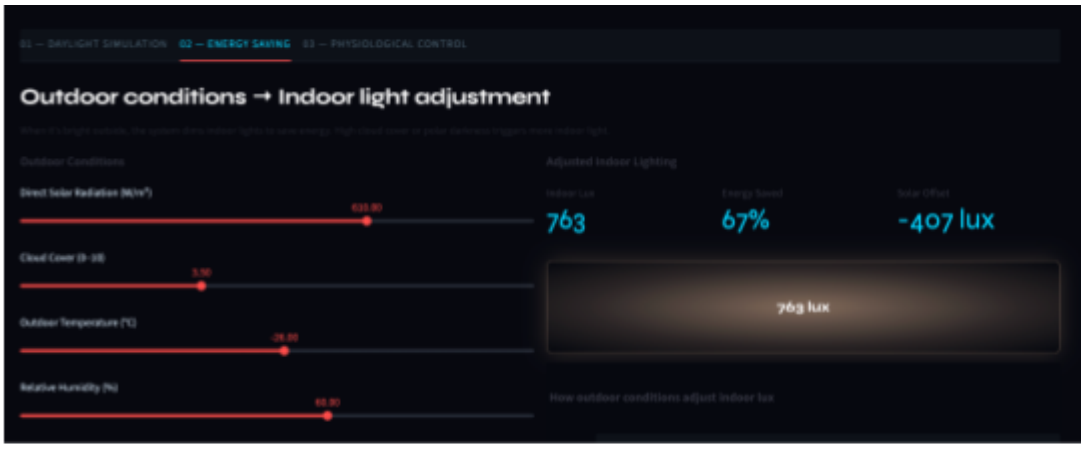

Fig. 21: Website showing energy saving tab

The physiological control tab works in a similar manner to the energy saving tab where the sliders of the features, such as heart rate, predict what the lighting response would be. Figure 22 displays a range of high stress parameters to the human body such as heart rate at 76 bpm, large pupil size at

6.10mm and similar factors which the model detects as tense and over-rides it to change the lighting to a lower lux at 637 lux and a warmer temperature at 2700k.

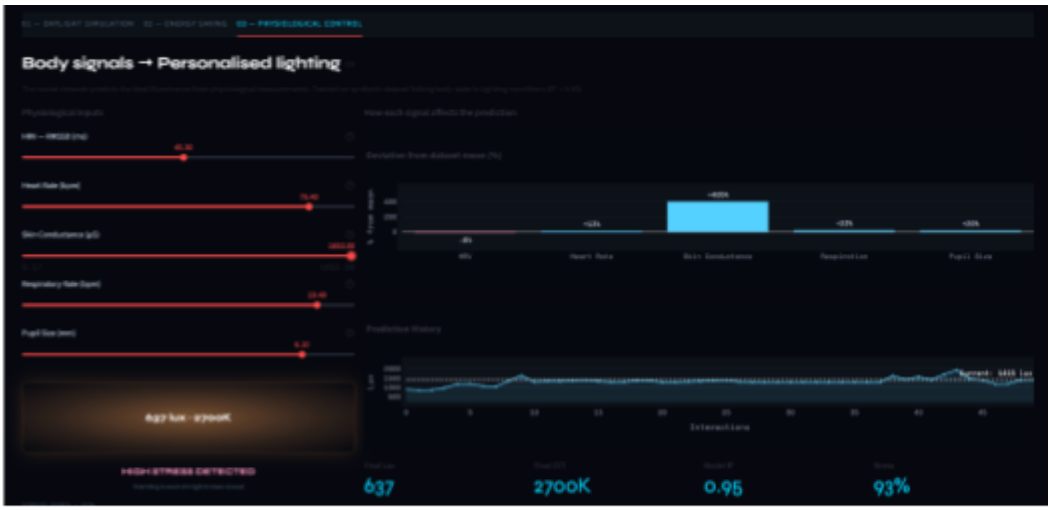

Fig. 22: Website showing physiological control tab

4.4.2 Visualisation of ML model containing Voronoi Design

While the initial iteration of the Streamlit interface was vital for validating the machine learning model's performance, it was necessary to move beyond numerical outputs to a spatialized representation. By integrating the 3D digital model of the container into the website, the application allowed for the simulation of real-time light changes. With the current setup, the face of the voronoi cells are affected by the weather data while the edges of the voronoi are controlled by the physiological data. By mapping the real time weather data on the face of the Voronoi tessellation, it allowed for a simulation of virtual skylights and windows. Conversely, the structural edges of the Voronoi functioned as a luminous skeleton, pulsing with the subtle changes through the occupant's physiological data. Figure 23 displays the simulation of the weather data onto the 3D model.

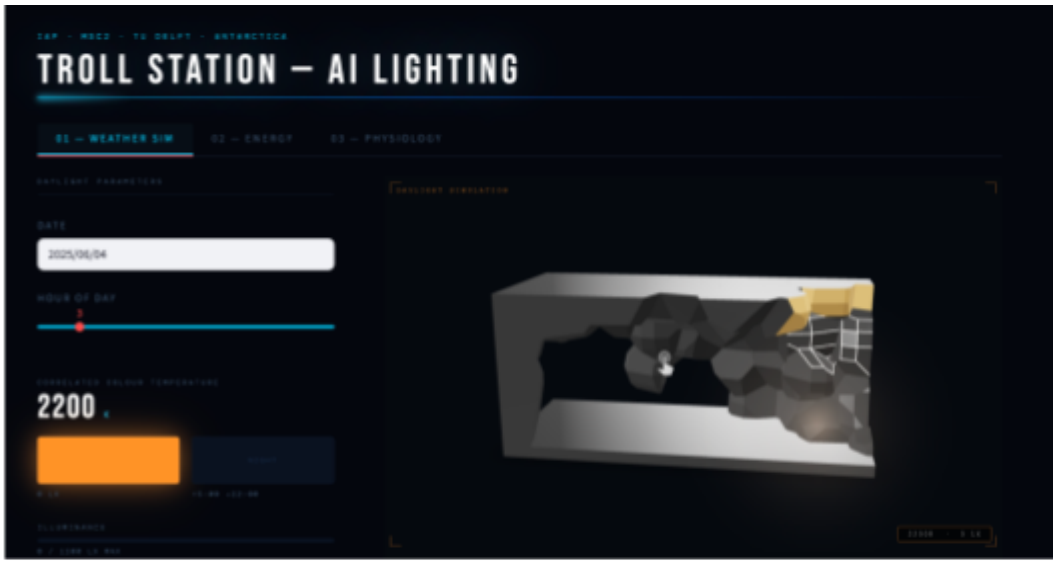

Fig. 23: Website showing integration of 3D model with weather, energy, and physiological tabs

4.4.3 Real time visualisation of ML model through wearable technology

To transition this predictive model from a theoretical simulation to a functioning architectural system, the python script was integrated with a wearable PPG (Photoplethysmography) sensing technology. PPG sensing refers to a non-invasive technology that uses a light source and photo detector at the surface of the skin to measure variables such as heart rate and pulse oximetry readings. [13] PPG sensors are often used in wearable watches such as Garmin, which was used for this study to facilitate a real time feedback loop where the user's heart rate directly modulated the lighting output. The immediate observation in the lighting changes in the 3D model integrated on the web app allows for the user to experience the container environment virtually.

Fig. 24: Website showing integration of Bluetooth to control 3D model in real time

Figure 24 displays the active heart rate of the participant and the lighting changes in real time. This was integrated through a Bluetooth Low Energy (BLE) communication protocol, a wireless technology designed for short range communication creating a bridge between the wearable technology and the control interface. [14] By reading the local JSON, JavaScript Object Notation, data streamed through the watch, the system reacts through shifting the lighting with minimal latency between one to ten seconds. This closed feedback loop allows for a more nuanced system design than the previous iteration where the sliders controlled the output.

4.5 Limitations of the ML model

Despite the highly predictable machine learning model and the successful integration of the Streamlit web interface for this study, there remain several limitations to this system. The first being the synthetic dataset of the physiological features used to train the model which do not reflect the

complex physiological fluctuations that occur in users that spend long periods of time in the polar regions. To make the model more accurate, data from occupants at the Troll Station will have to be collected for a certain period of time to reflect their physiological needs in the future.

Another limitation of the model is its lack of contextual awareness regarding physiological triggers. Because the system primarily relies on a user's heart rate or skin conductance, which can be easily measured by wearable technology, it cannot distinguish activities or mental state of the user causing the system to incorrectly recognize and change the lighting. For example, an elevated heart rate can indicate various conditions, such as physical exercise, excitement, stress, or caffeine intake, which may cause the model to over-ride the lighting and simulate an environment of relaxation instead. Activity recognition is quite an important factor and is currently absent from the model. In a future study, activity recognition could be integrated with the use of sensors and cameras inside the container to create a more nuanced lighting model.

Furthermore, another limitation is the integration of both the weather and physiological data together which may cause a conflict between the two causing circadian disruptions. For example, if it is noon and the sun is bright, creating a high lux and cooler CCT in the container, however, the occupant is experiencing high stress, the system might try to dim the lighting and create a warmer environment to calm the user down. This dispute between the two data points might disrupt the user's circadian rhythm where high intensity blue lighting is needed to maintain their biological clock. The model is currently lacking a hierarchy between the two systems which might be complicated to establish.

While these limitations can fine-tune the machine learning model, this study establishes an initial experimental methodology to create a more personalized lighting system to improve the occupant experience in the polar regions.

5. Conclusion & Limitations

5.1 Limitations and Future work

The system's reliance on localized data such as environmental inputs and physiological inputs, further improve its responsiveness. Rather than imposing a fixed spatial configuration, the design adapts in real time, allowing lighting and spatial design to respond dynamically to both external conditions and user needs. This is particularly significant in the extreme and isolated context of Troll Station, where conventional static systems fail to give a convincing answer to the fluctuating environmental conditions and human well-being requirements.

However, some limitations remain. First, the system's performance is highly dependent on the quality and reliability of input data. Inaccurate environmental or physiological data could lead to inappropriate lighting responses.
Second, while the geometric framework is flexible, its translation into physical construction, particularly environments like Troll Station, remains a challenge. Issues related to material durability, fabrication precision, and long-term maintenance must be further explored to ensure that the computational model can be realistically and sustainably implemented.
Additionally, the use of a Voronoi-based system introduces its own set of constraints. Voronoi geometries can produce irregular, fragmented, and non-uniform cell configurations. This can lead to increased material waste, complex joints, and challenges in integrating building systems such as structure, insulation, and services.
Finally, the current implementation focuses primarily on spatial distribution and lighting adaptation, leaving other critical environmental factors such as acoustics, thermal comfort, and air quality relatively underexplored. A more integrated approach of these parameters is necessary to fully realize a responsive and habitable environment.

5.2 Conclusion

This research demonstrates how the integration of D2RP and D2RO provides a powerful response to the spatial and environmental constraints of the Troll Station. By combining a Voronoi-based spatial system with an orthogonal grid with the help of a buffer zone, the project successfully negotiates between adaptivity and control. This approach enables the generation of different spatial arrangements while maintaining geometric coherence and constructability, effectively addressing the limited, rigid, and resource-constrained interior of the station.

References

[1] University of Bristol, “What is a Voronoi diagram?,” School of Mathematics, University of Bristol. [Online]. Available: https://www.bristol.ac.uk/maths/fry-building/public-art-strategy/what-is-a-voronoi-diagram/

[2] Bellelli F, “The fascinating world of Voronoi diagrams,” TDS Archive / Medium, Apr. 2, 2022. https://medium.com/data-science/the-fascinating-world-of-voronoi-diagrams-da8fc700fa1b

[3] Vitaterna MH, Takahashi JS, Turek FW, “Overview of circadian rhythms,” *Alcohol Research & Health*, vol. 25, no. 2, pp. 85–93, 2001. https://pmc.ncbi.nlm.nih.gov/articles/PMC6707128/

[4] Arendt J, “Biological rhythms during residence in polar regions,” *Chronobiology International*, vol. 29, no. 4, pp. 379–394, May 2012. https://pmc.ncbi.nlm.nih.gov/articles/PMC3793275/

[5] Petrowski K, Mekschrat L, Bührer S, Siepmann M, Albus C, Schmalbach B, “Effects of post-awakening light exposure on heart rate variability in healthy male individuals,” Applied Psychophysiology & Biofeedback, vol. 48, pp. 311–321, 2023. https://doi.org/10.1007/s10484-023-09581-7

[6] Najjar E, Breesam A, “Supervised Machine Learning: A Brief Survey of Approaches,” Al-Iraqia Journal of Scientific Engineering Research, vol. 2, pp. 71–82, 2023. https://doi.org/10.58564/IJSER.2.4.2023.121

[7] “Climate Data for the Netherlands,” One Building Climate Data, https://climate.onebuilding.org/WMO_Region_6_Europe/NLD_Netherlands/index.html

[8] Xue Y, “An overview of overfitting and its solutions” Journal of Physics: Conference Series, vol. 1168, 022022, 2019. https://doi.org/10.1088/1742-6596/1168/2/022022

[9] Feng X, Ma G, Su SF, Huang C, Boswell MK, Xue P, “A multi-layer perceptron approach for accelerated wave forecasting in Lake Michigan,” Ocean Engineering, vol. 211, pp. 107526, 2020. https://doi.org/10.1016/j.oceaneng.2020.107526

[10] Du KL, Zhang R, Jiang B, Zeng J, Lu J, “Understanding machine learning principles: Learning, inference, generalization, and computational learning theory,” Mathematics, vol. 13, no. 3, pp. 451, 2025. https://doi.org/10.3390/math13030451

[11] Gao J, “R-squared (R^2) – How much variation is explained?,” Research Methods in Medicine & Health Sciences, vol. 5, no. 7, 2023. https://doi.org/10.1177/26320843231186398

[12] Miller C, Portlock T, Nyaga DM, O’Sullivan JM, “A review of model evaluation metrics for machine learning in genetics and genomics,” Frontiers in Bioinformatics, vol. 4, pp. 1457619, 2024. https://doi.org/10.3389/fbinf.2024.1457619

[13] Castaneda D, Esparza A, Ghamari M, Soltanpur C, Nazeran H, “A review on wearable photoplethysmography sensors and their potential future applications in health care,” International Journal of Biosensors & Bioelectronics, vol. 4, no. 4, pp. 195–202, 2018. https://doi.org/10.15406/ijbsbe.2018.04.00125

[14] Gomez C, Oller J, Paradells J, “Overview and evaluation of Bluetooth Low Energy: An emerging low-power wireless technology,” Sensors (Basel), vol. 12, no. 9, pp. 11734–11753, 2012. https://doi.org/10.3390/s120911734